SCIENCE CHINA
Technological Sciences

•Article•

March 2020 Vol.63 No.3: 520–527
https://doi.org/10.1007/s11431-019-1434-y

In-situ lunar dust deposition amount induced by lander landing in Chang'E-3 mission

ZHANG HaiYan[1], WANG Yi[1*], CHEN LiPing[2], ZHANG He[2*], LI CunHui[1], ZHUANG JianHong[1], LI DeTian[1], WANG YongJun[1], YANG ShengSheng[1], LI XiongYao[3] & WANG WeiDong[4]

[1] *Science and Technology on Vacuum Technology and Physics Laboratory, Lanzhou Institute of Physics, Chinese Academy of Space Technology, Lanzhou 730000, China;*
[2] *Beijing Institute of Physics, Chinese Academy of Space Technology, Beijing 100094, China;*
[3] *Center for Lunar and Planetary Sciences, Institute of Geochemistry, Chinese Academy of Sciences, Guiyang 550081, China;*
[4] *School of Mechano-Electronic Engineering, Xidian University, Xi'an 710071, China*

Received February 2, 2019; accepted August 12, 2019; published online January 2, 2020

China first *in-situ* lunar dust experiment is performed by a lunar dust detector in Chang'E-3 mission. The existed dust (less than 20 μm in diameter) properties, such as levitation, transportation and adhesion, are critical constraints for future lunar exploration program and even manned lunar exploration. Based on the problems discussed above, the *in-situ* lunar dust detector is originally designed to characterize dust deposition properties induced by lander landing as a function of environmental temperature, solar incident angle and orbit short circuit current on the northern Mare Imbrium, aiming to study lunar dust deposition properties induced by lander landing in depth. This paper begins with a brief of introduction of Chang'E-3 lunar dust detector design, followed by a series of experimental analysis of this instrument under different influencing factors, and concludes with lunar dust mass density deposition amount observed on the first lunar day is about 0.83 mg/cm^2, which is less than that observed in Apollo 11 mission because the landing site of Chang'E-3 has the youngest mare basalts comparing with previous Apollo and lunar landing sites. The young geologic environment is less weathered and thus it has thinner layer of lunar dust than Apollo missions'; hence, the amount of kicked-up lunar dust in Chang'E-3 mission is less than that in Apollo 11 mission.

***in-situ* lunar dust experiment, Chang'E-3 mission, unnatural mechanisms, lunar dust deposition amount**

Citation: Zhang H Y, Wang Y, Chen L P, et al. *In-situ* lunar dust deposition amount induced by lander landing in Chang'E-3 mission. Sci China Tech Sci, 2020, 63: 520–527, https://doi.org/10.1007/s11431-019-1434-y

1 Introduction

Chinese Chang'E-3 mission, as part of the second phase of Chinese Lunar Exploration Program (CLEP) and including orbiting and landing, was launched at 17:30 UTC on 1 December 2013 (01:30 local time on 2 December) by adopting a Long March 3B rocket flying from Launch Complex 2 at the Xichang Satellite Launch Centre in the southwestern province of Sichuan and its successful landing was on the northern Mare Imbrium of the lunar nearside (340.49°E, 44.12°N) on December 14, 2013. The lunar dust detector, with scientific objectives to characterize lunar dust deposition property, is carried by Chang'E-3 lander even aiming at future improvement design for mechanical structure, astronaut suit, or even at investigation on lunar surface geology.

During Apollo exploration period, it is found that lunar dust and its adhesion to astronaut space suit, hardware, mechanical seals and equipment will lead to occasional and

*Corresponding authors (email: wangyi9601@163.com; zhanghe_maoqiu@163.com)

inescapable difficulties in exploring lunar surface [1–3]. From then on, the main attention of lunar scientific researchers is given to characteristics of dust through simulation, laboratory experiment and relative space lunar detector, which are much important for understanding lunar dust composition, adhesion, levitation, and transport properties using amount of simulation and ground experimental methods and several kinds of detectors [4–7]. Among all researches about lunar dust, however, the space scientific detectors about *in-situ* lunar dust investigation are only onboard of Apollo 11, 12, 14, 15 and 17 missions, the instrument named Lunar Dust Experiment (LDEX) onboard the Lunar Atmosphere and Dust Environment Explorer (LADEE) mission and Chang'E-3 mission until now.

The lunar dust detectors designed for Apollo missions, with altitude of about 100 cm above lunar surface, are mainly used for dust sunrise-driven movement investigations and relative lunar dust particle accumulation rate at different time obtained by Apollo 11, 12, 14, and 15. A series of influential research achievements are published by professor O'Brien's team [8–10] in recent years and the results reveal part of levitation properties of lunar dust in case of natural mechanism and part of deposition properties of lunar dust induced by lunar module descent and ascent stages. LDEX instrument achieved lunar dust environmental measurement covering an altitude range of about 3–250 km far from the lunar surface, during which lunar dust particle mass existing in lunar exosphere is recorded as a function of local time and position of the Moon with respect to the magnetosphere of the Earth [11,12].

Specifically, the lunar dust is one of the highest priority issues that should be solved not only from a physical prospective, but also for future human or other advanced style lunar exploration. Unfortunately, both Apollo mission and LDEX mission focus more on lunar dust own parameters of dust charge, speed and mass and characters of dust transportation, levitation properties under natural mechanism, which may not offer comprehensive information about lunar dust other properties under unnatural mechanism that is of great importance for future manner mission. Although Apollo mission reveals the fact that how rocket stir up clouds of lunar dust, the Apollo missions' landing sites are limited and are different from Chang'E-3 landing site. Thus, more sufficient detection data about lunar dust properties at different Moon area is needed to reveal lunar dust distribution, levitation and transport properties in depth. Based on above purposes, China designs a highly sensitive lunar dust detector (LDD) attempting to investigate dust deposition property induced by the landing of lunar lander in Chang'E-3 mission with altitude of 205 cm over lunar surface, that is to say, this instrument makes effort to assess the amount of lunar dust that may be expected to accumulate on LDD as a result of lander landing in Chang'E-3 mission.

2 Overview of Chang'E-3 lunar dust detector design

Chang'E-3 lunar dust detector (LDD), a high-performance dust instrument, is composed of two parts: solar cell probe (SCP) acts as sensor head and its corresponding electronic box that includes A/D circuit, communication circuit, control circuit and storage circuit. Their mutual working relationship is shown in Figure 1. In the following chapters, the detail description about this detector will be presented. According to the existed literature [13–15], the deposition of lunar dust on the surface of solar cell will be at risk of performance reductions on its parameters of short-current (I_{sc}) and open-voltage (V_{oc}). Based on this principle, SCP is applied to detect lunar dust mass accumulation property with a wide range in the process of lunar lander landing and lunar rover movement. In this paper, SCP-LDD is used to simplify this instrument full name.

The SCP-LDD, as shown in Figure 2, is mounted on the front left corner of the lander and has altitude of 205 cm.

The sensor head of SCP-LDD mainly contains three parts, namely a tri-junction GaInP/GaAs/Ge solar cell with size of 30 mm (A_w) in width and 40 mm (A_l) in length, a shell box to install and support solar cell and an electric coupler to realize signal measurement and transmission with electric box. The SCP-LDD electric box contains four parts: Analog to Digital (A/D) signal module, communication module, control module and storage module. The output accuracy of sensor head is 0.1 mA for SCP output current (I_{sc}) to reveal the reality of lunar dust deposition property information. The powder unit supplies 29 V voltage to this instrument. The LDD instrument picture is shown in Figure 3. The temperature, which is one of an important environmental factor on SCP-LDD output of sensor head input in lunar environment measurement of this instrument, is applied to monitor whether local lunar real-time temperature of the solar cell probe works in the normal range from –180°C to +120°C or not, in other words, if lunar local environmental temperature beyond this range, relative control circuit will close SCP-LDD to protect it from hostile environment.

3 Experimental analysis of environmental influencing factors on SCP-LDD performance

According to the preliminary results [16–18], dust deposition is a main factor but not the only factor affecting SCP-LDD performance decrease. There are numbers of environmental factors which influenced the performance of SCP-LDD such as solar light intensity, ambient temperature, solar incident angle. Among all influencing factors listed above, one of the major factors degrading the SCP-LDD output performance is still lunar dust deposition induced by Chang'E-3 lander

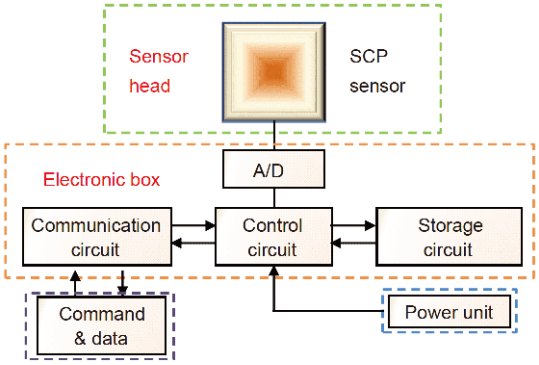

Figure 1 (Color online) The Chang'E-3 lunar dust detector schematic program.

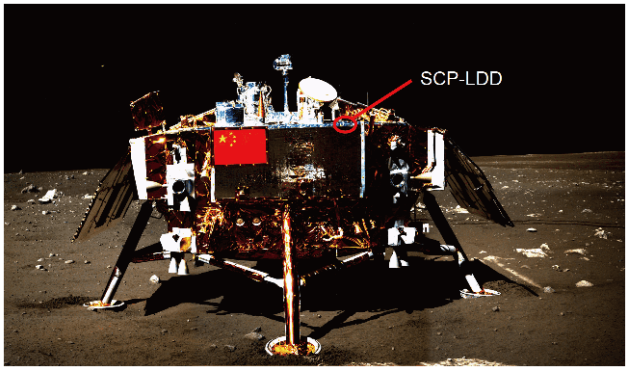

Figure 2 (Color online) The location of lunar dust detector on Chang'E-3 lander.

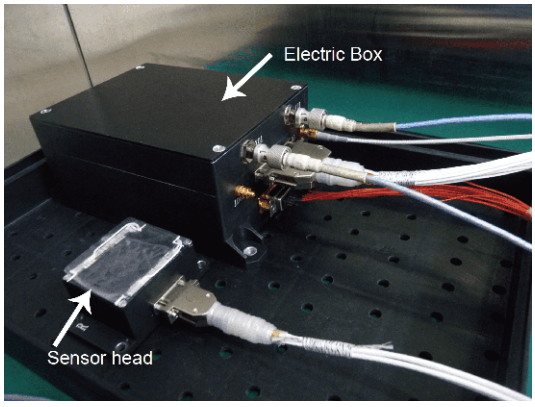

Figure 3 (Color online) The main geometry design of sensor head and its electric box.

landing; hence, this instrument is utilized to measure dust deposition properties under different environmental factors here. In order to well know how different factors affect SCP-LDD performance, a set of experiments are designed to demonstrate the detailed relationship between ambient temperature, solar light intensity, solar incident angle and lunar dust deposition and SCP-LDD performance, which will enable to verify the validity and accuracy of space lunar dust deposition data.

3.1 Experimental system

The experimental system is set up as shown in Figure 4, which is comprised of a solar simulator, an elevator, vacuum chamber, and corresponding fixed devices. The simulator is calibrated to 1-sun condition (AM0: 1351 W/m^2). The micro-balance is placed the outside of vacuum and its precision adopted in the experiment has a minimum measurable weight of 0.1 μg. The elevator range is from –90° to +90° with accuracy of 1°. The power unit supplies 29 V voltage to this detector. In this work, the initial I_{sc} of SCP-LDD is 198.6 mA and it remains unchanged when solar simulator light incident angle is 0°, lunar dust deposition density is 0 g/cm^2 and the ambient temperature is 25°C. During the whole experiment, the solar intensity is fixed to the level of 1351 W/m^2 and this level is maintained throughout the whole test program. The major purpose of this experiment is to assess the amount of dust accumulation on SCP-LDD at different time. The existed approach for this kind of calculation is to know the influence of single parameter on short circuit current of SCP-LDD and finally subtract the value of each current effect from final current to calculate mass deposition [1,11,16,18].

3.2 Effect of temperature

As we all know, I_{sc} output of solar cell is sharply sensitive to its ambient temperature [19–20]. The SCP-LDD temperature coefficient (α) is calibrated to work at different temperatures and the result confirms that its value is 0.01 mA cm^{-2} °C^{-1}, which is offered by No.18 Research Institute, China Electronics Technology Group Corporation. Thus, the relationship between ΔI_{scT} and temperature is as follows:

$$\Delta I_{scT} = \alpha \times A \times \int_{25}^{T} \mathrm{d}T, \tag{1}$$

where I_{scT} is short circuit current when solar incident angle is 0° and dust deposition density is 0 mg/cm^2, α =0.01 mA cm^{-2} °C^{-1} is temperature coefficient, A=A_w×A_l =12 cm^2 is solar cell area, T is ambient temperature (°C).

By integrating both sides of eq. (1), we can obtain ΔI_{scT} as following:

$$\Delta I_{scT}=0.01 \times 12 \times \Delta T = 0.12(T-25). \tag{2}$$

It can be concluded from eq. (2) that I_{scT} linearly increases with the increase of ambient temperature.

3.3 Effect of solar incident angle

In general, solar incident angle (θ) is a factor that has great influence on solar cell output. As it is a well-known thing that the relationship between the short circuit current of solar cell and incident sunlight angle is

$$I_{sc\theta} = I_0 \times \cos\theta, \tag{3}$$

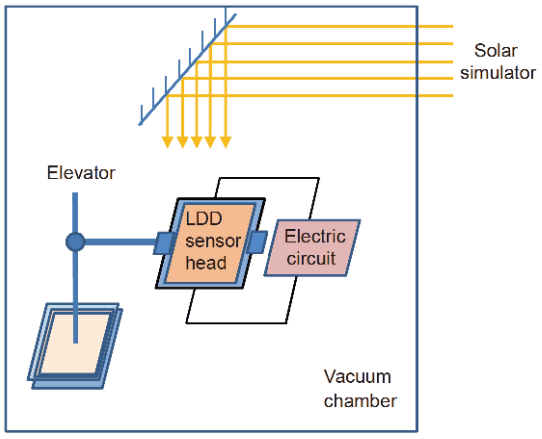

Figure 4 (Color online) SCP-LDD schematic diagram of experimental system.

where I_0 is short circuit current when solar angle is 0°, dust deposition density is 0 mg/cm^2 and ambient temperature is 25°C.

However, with the increase of incident angle, the relationship between the output current and incident sunlight angle is not cosine function any more, which is a universal phenomenon for solar cell. Figure 5 obviously shows an empirical relation for incident angle coefficient (P) as a function of solar incident angle (θ) and incident angle sharply decreases as incident angle is over 50°. Their nonlinear fitting relationship is written as

$$P = 1.00526 - 3.102 \times 10^{-5} \times e^{(\theta/8.662)}, \quad (4)$$

where P is incident angle coefficient.

By combining the eqs. (3) and (4), incident angle coefficient (η_θ) can be defined as follows:

$$\eta_\theta = \cos\theta \times P = \cos\theta \times (1.00526 - 3.102 \times 10^{-5} \times e^{(\theta/8.662)}). \quad (5)$$

3.4 Effect of lunar dust deposition

The main task of this experiment is to obtain the characteristic of the SCP-LDD I_{sc} when dust particles are deposited on its surface at varying densities. The steps taken for conducting this experiment term are as follows. Firstly, the lunar dust samples are weighed by micro-balance. Secondly, the lunar dust samples are carefully transferred to solar cells of SCP-LDD in a very clean condition uniformly. Finally, I_{sc} values of the detector are measured in condition of different lunar dust samples' mass density. Lunar dust samples are offered by the Institute of Geochemistry Chinese Academy named CLDs-i, whose properties are high similar to real lunar dust to do scientific exploration [21,22]. In order to assess the reduction in the short circuit current of this detector with lunar dust deposition, the current is plotted against the simulant lunar dust deposition density and the result is shown in Figure 6.

It can be easily obtained that the short current reduction in Figure 6 is not liner with dust deposition density (x) and their nonlinear fitting result is

$$I_{scx} = 233.39686e^{(-x/6.84262)} - 41.26008, \quad (6)$$

where x denotes dust deposition density (mg/cm^2), I_{scx} is short circuit current of SCP-LDD when ambient temperature is 25°C, solar incident angle is 0°. It should be noticed that I_{scx} decreases empirically with increase in dust accumulation density (x).

Further,

$$\Delta I_{scx} = I_{scx} - I_0 = 233.39686^{(-\Delta x/6.84262)} - 41.26008 - I_0. \quad (7)$$

The above experiments have offered direct effects of ambient temperature, solar sunlight incident angle, and dust deposition density on short circuit current of SCP-LDD, which is able to make quantitative analysis for orbit data. In order to obtain the short circuit current that only be affected by lunar dust mass deposition density, we should subtract I_{scT}

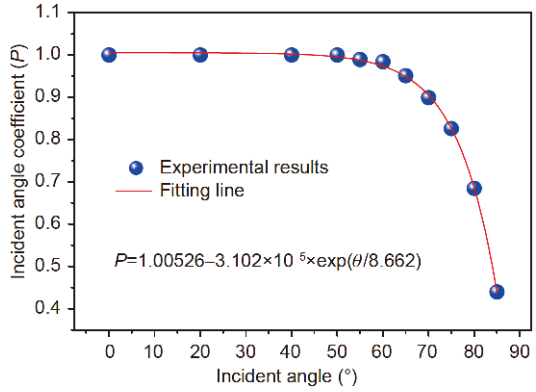

Figure 5 (Color online) Variation of incident angle coefficient with incident angle.

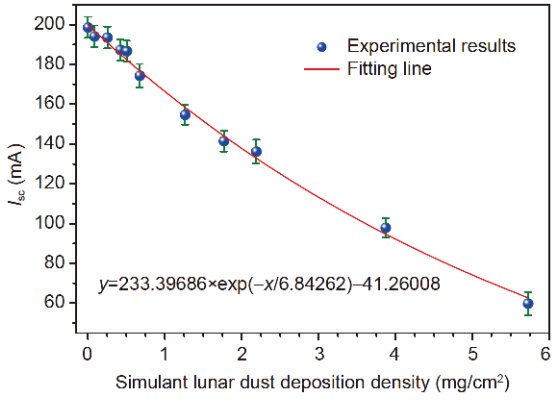

Figure 6 (Color online) Variation of short circuit current with dust deposition density.

and $I_{sc\theta}$ from orbit short circuit current. However, the corresponding short circuit current of the solar incident angle coefficient η_θ is the current that has subtracted temperature factor and mass deposition density factor. Therefore, combining the experimental results in eqs. (2), (5) and (6), the orbit short circuit current at different local time should be written as

$$I_i = (I_0 - \Delta I_{scTi} - \Delta I_{scxi}) \times \eta_{\theta i}, \tag{8}$$

where I_0=198.6 mA corresponding its dust deposition mass of 0 mg/cm^2, I is output short circuit current of SCP-LDD on condition of different ambient temperatures, solar incident angles and lunar dust deposition densities, i denotes time point at different earth daytime points.

Further,

$$\begin{aligned}\Delta I_{scxi} &= I_0 - \Delta I_{scTi} - I_i/\eta_{\theta i} = I_{scxi} - I_0 \\ &= 198.6 + 0.12T_i + 3 \\ &\quad - I_i/\cos\theta_i(1.00526 - 3.102e^{(\theta_i/8.662)} \times 10^{-5}),\end{aligned} \tag{9}$$

$$\begin{aligned}\Delta I_{scxi} &= I_{scxi} = I_{scTi} + I_i/\eta_{\theta i} \\ &= 0.12T_i - 3 + I_i/\cos\theta_i(1.00526 \\ &\quad - 3.102e^{(\theta_i/8.662)} \times 10^{-5}).\end{aligned} \tag{10}$$

Thus, lunar dust deposition density Δx can be calculated by solving eq. (10).

4 Results and analysis

The lunar dust detector was carried by Chang'E-3 lander which landed on the northern Mare Imbrium at 21:11 BJT (UTC +8h) on December 14, 2013 successfully, performing its first operation at 3 o'clock BJT (UTC +8h) on December 15 successfully. The first lunar day for SCP-LDD corresponding to its relative earth daytime was over the period December 15–24, 2013. Upon working, SCP-LDD started to make measurements of local sunlight intensity, incident solar angle and output current and the historical curves of the three parameters as a function of time on the first lunar day are illustrated in Figure 7, from which it can be obviously found a fact that local sunlight intensity and effective sunlight intensity pushed on SCP-LDD increase at first and then decrease ranging from about 530 W/cm^2 to 1000 W/cm^2. It is about 2° angle between solar cell of SCP-LDD and local lunar surface that makes local sunlight intensity different from effective sunlight intensity on solar cell. The solar incident angle on solar cell firstly decreases and then increases and it varies with a certain range from about 44° to 67°, which is opposite to sunlight intensity variation trend. On December 20, 2013, the local sunlight intensity reaches its peak value but incident angle is its minimum value, which indicates that this earth day corresponds noon time of the first lunar day.

Variation of ambient temperature at different daytime on the first lunar day is shown in Figure 8, where it can be found that the maximum temperature is about 55°C but the minimum temperature is only about 3°C and this variation curve has similar trend with Figure 7. The maximum temperature point occurs on the fifth earth daytime of December 20, indicating that the parameters observed by SCP-LDD are much effective to analyze dust deposition density to further reveal how Chang'E-3 lander induces lunar dust movement when it landing. What SCP-LDD also concerns about is overheating, leading to damage of this detector. Fortunately, there has no temperature jump occurring in Figure 8, that is to say, observed data on the first lunar day is effective.

In Figure 9, it obviously illustrates the lunar dust mass density deposition property at different earth daytimes on the first lunar day after SCP-LDD performance. On working, the lunar time is not early morning but long after sunrise, a fact is known through SCP-LDD actual working time corresponding to instantaneous solar incident angle of about 60°. The reason why lunar dust deposition on the first earth daytime of

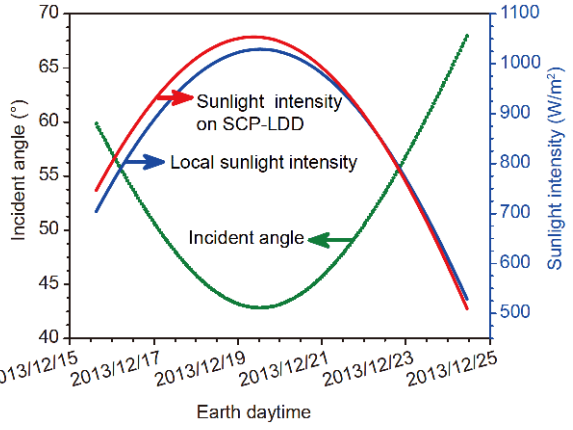

Figure 7 (Color online) The historical curves of local sunlight intensity, sunlight intensity on solar cell and solar incident angle as a function of earth daytime on the first lunar day.

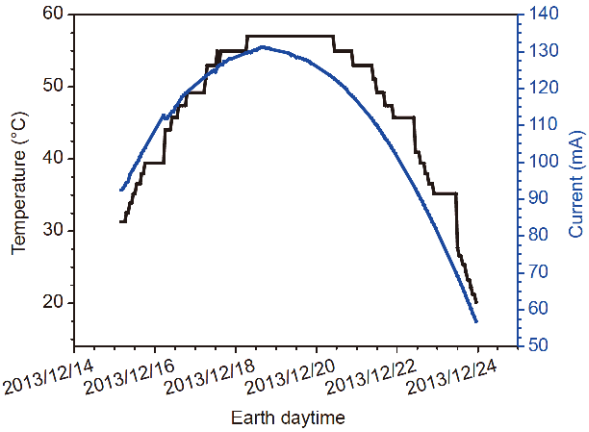

Figure 8 (Color online) Variation of ambient temperature with earth daytime on the first lunar day.

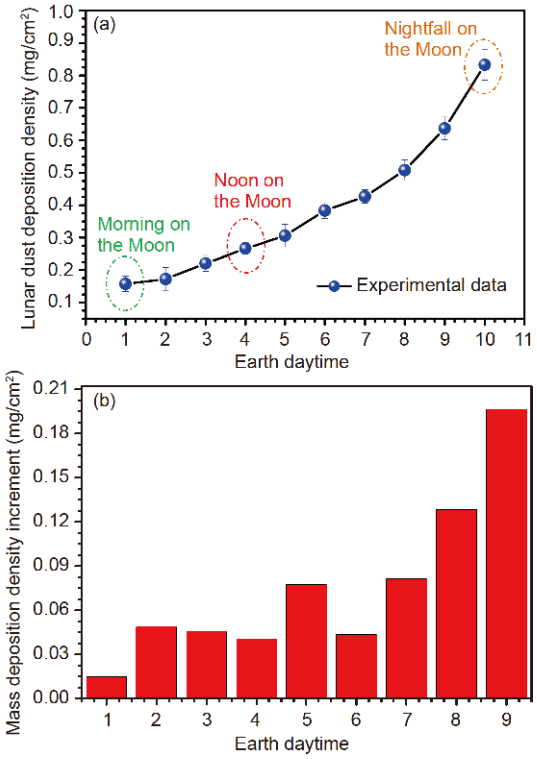

Figure 9 (Color online) Lunar dust mass deposition density property on the first lunar day (the errors bars in Figure 9(a) denote the standard deviation of lunar dust mass deposition density. Lunar dust deposition rate in Figure 9(b) is defined as follows: the lunar dust mass deposition density in the first and the second earth daytime are A and B, respectively, then the deposition increment between the two daytimes is B-A).

the first lunar day, shown in Figure 9(a), is not 0 mg/cm^2 but 0.157 mg/cm^2 is that SCP-LDD boot time is later than landing time, during which part of lunar dust resulted from lander has deposited on it. It should be noticed that the final deposition properties of SCP-LDD in this experiment are based on neglect of space radiation effect on it for only a lunar day, attributing to its excellent radiation resistance as demonstrated by space solar cell relative radiation resistance experiments based on Apollo missions and other lunar exploration experiments [23–25]. Moreover, it also can be seen from Figure 9(a) that, with time goes on, lunar dust mass deposition density gradually increases with obvious fluctuation and its total deposition density in this experiment is about 0.833 mg/cm^2, corresponding to short circuit current output decrease of 16.721% on the first lunar day. It also can be inferred from Figure 9(b) that lunar dust mass deposition density increment fluctuates every earth daytime and the maximum value of it happens on the last earth daytime.

Exhaust gases from descent lander in Chang'E-3 mission is the most important factor to splash lunar dust existed on landing surface. Apollo astronauts who landed on the Moon saw lunar dust was kicked up by lander exhausts of its descent stage for the first time [1,26]. These kicked up lunar dust particles had great harm to hardware and astronauts future mission. Lunar dust detector is an innovative instrument to continuously explore dust properties affecting further lunar investigation. Until now, the existed lunar dust accumulation properties affected by lander descent, lunar rover movement or human activities are much few because of few opportunities of lunar exploration. SCP-LDD designed here is applied to investigate lunar dust accumulation amount resulting from lander exhaust gas to guide lunar dust preliminary protection in future missions.

Until now, only observation data obtained from lunar dust detector in Apollo 11, 12 and 14 missions have similarity with our results based on similar objective to some degree. Decreases in outputs of the 3 horizontal solar cells on the Apollo 11 lunar dust detector are 0%, 7% and 17% respectively [1,27]. Unfortunately, direct measurement of Apollo 12 and Apollo 14 observed unexpected results of cleansing effects on hardware resulting from lunar module rocket exhausts. The final decrease in output of Apollo lunar dust detector was only about 6 h after lunar module ascent, during which the decrease in SCP-LDD output was only 5.927% corresponding to its mass deposition density of 0.157 mg/cm^2, which was less than that measured in Apollo 11. This phenomenon can be illustrated by a fact that the landing site of Chang'E-3 has the youngest mare basalts comparing with previous Apollo and lunar landing sites, which indicates that it is less weathered and its deposition amount in Chang'E-3 mission is less than that measured in Apollo 11 mission [28–30]. However, we draw attention here to the reality that lunar dust detector's output still continuously decrease after 6 hours after ascent because dust accumulation over the first 3 lunar dust days amounted to about 30% of the total accumulated over 6 years on horizontal solar cell demonstrated in Apollo mission [31]. If we assume that other factors, such as local lunar environmental parameters, will not change, the total dust mass deposition of lunar dust at descent stage during landing in Chang'E-3 mission is less than that observed in Apollo 11 mission at ascent stage.

Holick's team [32] analyzed and provided upper limit of order 100 μg/(cm^2 yr) caused by natural factors such as electrostatic transport and micrometeoroid collision, which is the first direct measured long-term lunar dust accumulation value to describe dust accumulation amount in Apollo missions on natural mechanism, such as dust electrostatic levitation and transport, and its amount is much less than that measured in Chang'E-3 mission because electrostatic force and collision force are much less than impact force caused by exhaust gases. The fluctuations observed in Figure 9(b) may be explained as follows: lunar dust particles' descent velocity are not constant actually due to their own properties such as different shapes, and cohesion and adhesion forces of themselves, in addition, a rover named Yutu released by lander and then began to move around Chang'E-3 lander on

the first lunar day and therefore its movements induced lunar dust around landing site depositing on SCP-LDD, which also makes dust deposition increase [33,34]. In general, lunar dust deposition on SCP-LDD is induced by two reasons: lander landing acting as a main factor and rover movement acting as a secondary factor. However, quantitative proportionality between the two factors is hard to analyze because of the absence of further rover movement speed data, lunar dust descent speed, splashed height and so on, which may be a part of interesting investigation for lunar dust in the subsequence missions. Fortunately Chang'E-4 mission will provide systematic data support about lunar dust and its relative data analysis will be reported in subsequent articles [35,36].

5 Summary

In summary, lunar dust detector SCP-LDD is designed to detect lunar dust deposition resulted from unnatural mechanisms of lander landing. After considering the effects of different factors such as ambient temperature, solar incident angle and lunar dust deposition on SCP-LDD output short circuit current, the relationship between lunar dust mass deposition increments and SCP-LDD output short circuit current decrement via subtracting relative output short circuit current value induced by other two factors according to quantitative results are measured in Sect. 3. In this mission, the amount of lunar dust deposition on the first lunar day is about 0.83 mg/cm^2 and its deposition is mainly induced by lander landing and maybe is induced by a minor factor of rover movement through analyzing the fluctuation of lunar dust deposition and rover movement route. By comparing dust deposition in this mission and Apollo 11 mission, it can be found that the deposition amount in this mission is less than that obtained in Apollo 11, which is caused by the reason that the landing site has the youngest geological age comparing with Apollo 11, thus, the existed lunar dust amount on lunar surface of this mission is less than that in Apollo 11 mission and finally has less amount of kicked-up lunar dust by lander.

This work was supported by the Beijing Institute of Spacecraft System Engineering, the National Natural Science Foundation of China (Grant No. 11605080), and the State Key Laboratory of Environmental Geochemistry for providing the simulant lunar dust.

1 O'Brien B J. Review of measurements of dust movements on the Moon during Apollo. Planet Space Sci, 2011, 59: 1708–1726
2 Wang X, Schwan J, Hsu H W, et al. Dust charging and transport on airless planetary bodies. Geophys Res Lett, 2016, 43: 6103–6110
3 Hou X, Fu H, Yang X, et al. Study on charging mechanism model of lunar dust for technology of particle removal from detector. In: Proceedings of the IEEE International Conference on Mechatronics and Automation (ICMA). Harbin: IEEE, 2016. 1513–1517
4 Kuznetsov I A, Zakharov A V, Dolnikov G G, et al. Lunar dust: Properties and investigation techniques. Sol Syst Res, 2017, 51: 611–622
5 Li L, Zhang Y T, Zhou B, et al. Dust levitation and transport over the surface of the Moon. Sci China Earth Sci, 2016, 59: 2053–2061
6 Jiang J, Zhao H, Wang L, et al. Analysis of influence factors on dust removal efficiency for novel photovoltaic lunar dust removal technology. Smart Mater Struct, 2017, 26: 125025
7 Horányi M, Szalay J R, Kempf S, et al. A permanent, asymmetric dust cloud around the Moon. Nature, 2015, 522: 324
8 O'Brien B. Overview of 14 discoveries 1969-2015 from Apollo measured movements of lunar dust. In: Proceedings of the EGU General Assembly Conference Abstracts. Vienna, 2016, 18. 1685
9 O'Brien B J, Hollick M. Sunrise-driven movements of dust on the Moon: Apollo 12 Ground-truth measurements. Planet Space Sci, 2015, 119: 194–199
10 O'Brien B J. Paradigm shifts about dust on the Moon: From Apollo 11 to Chang'e-4. Planet Space Sci, 2018, 156: 47–56
11 Janches D, Pokorný P, Sarantos M, et al. Constraining the ratio of micrometeoroids from short- and long-period comets at 1 AU from LADEE observations of the lunar dust cloud. Geophys Res Lett, 2018, 45: 1713–1722
12 Poppe A R, Halekas J S, Szalay J R, et al. LADEE/LDEX observations of lunar pickup ion distribution and variability. Geophys Res Lett, 2016, 43: 3069–3077
13 Saidan M, Albaali A G, Alasis E, et al. Experimental study on the effect of dust deposition on solar photovoltaic panels in desert environment. Renew Energy, 2016, 92: 499–505
14 Gholami A, Khazaee I, Eslami S, et al. Experimental investigation of dust deposition effects on photo-voltaic output performance. Sol Energy, 2018, 159: 346–352
15 Lu H, Zhao W. Effects of particle sizes and tilt angles on dust deposition characteristics of a ground-mounted solar photovoltaic system. Appl Energy, 2018, 220: 514–526
16 Said S A M, Hassan G, Walwil H M, et al. The effect of environmental factors and dust accumulation on photovoltaic modules and dust-accumulation mitigation strategies. Renew Sustain Energy Rev, 2018, 82: 743–760
17 Gupta V, Raj P, Yadav A. Investigate the effect of dust deposition on the performance of solar PV module using LABVIEW based data logger. In: Proceedings of the IEEE International Conference on Power, Control, Signals and Instrumentation Engineering (ICPCSI). Chennai: IEEE, 2017. 742–747
18 Chikate B V, Sadawarte Y. The factors affecting the performance of solar cell. Int J Comput Appl, 2015, 1: 0975-8887
19 Yang W C, Lo C, Wei C Y, et al. Cell-temperature determination in InGaP-(In)GaAs-Ge triple-junction solar cells. IEEE Electron Device Lett, 2011, 32: 1412–1414
20 Umachandran N, TamizhMani G S. Effect of spatial temperature uniformity on outdoor photovoltaic module performance characterization. In: Proceedings of the IEEE 43rd Photovoltaic Specialists Conference (PVSC). Portland: IEEE, 2016. 2731–2737
21 Tang H, Li X, Zhang S, et al. A lunar dust simulant: CLDS-i. Adv Space Res, 2017, 59: 1156–1160
22 Sun Y, Liu J, Zhang X, et al. Mechanisms involved in inflammatory pulmonary fibrosis induced by lunar dust simulant in rats. Environ Toxicol, 2019, 34: 131–140
23 O'Brien B J, Hollick M. Sunrise-driven movements of dust on the Moon: Apollo 12 Ground-truth measurements. Planet Space Sci, 2015, 119: 194–199
24 Ochoa M, Yaccuzzi E, Espinet-González P, et al. 10 MeV proton irradiation effects on GaInP/GaAs/Ge concentrator solar cells and their component subcells. Sol Energy Mater Sol Cells, 2017, 159: 576–582
25 Zhu L, Yoshita M, Nakamura T, et al. Characterization and modeling of radiation damages via internal radiative efficiency in multi-junction

solar cells. In: Proceedings of the Physics, Simulation, and Photonic Engineering of Photovoltaic Devices V. International Society for Optics and Photonics. San Francisco, 2016. 9743: 97430U
26 O'Brien B J. Paradigm shifts about dust on the Moon: From Apollo 11 to Chang'e-4. Planet Space Sci, 2018, 156: 47–56
27 O'Brien B. Direct active measurements of movements of lunar dust: Rocket exhausts and natural effects contaminating and cleansing Apollo hardware on the Moon in 1969. Geophys Res Lett, 2009, 36: L09201
28 Xiao L, Zhu P, Fang G, et al. A young multilayered terrane of the northern Mare Imbrium revealed by Chang'E-3 mission. Science, 2015, 347: 1226–1229
29 Fa W, Zhu M H, Liu T, et al. Regolith stratigraphy at the Chang'E-3 landing site as seen by lunar penetrating radar. Geophys Res Lett, 2015, 42: 10179–10187
30 Hu B, Wang D, Zhang L, et al. Rock location and quantitative analysis of regolith at the Chang'e 3 landing site based on local similarity constraint. Remote Sens, 2019, 11: 530
31 Gold T. Lunar-Surface Closeup Stereoscopic Photography. Apollo 14: Preliminary Science Report. NASA SP-272, Washington DC, 1971. 239
32 Hollick M, O'Brien B J. Lunar weather measurements at three Apollo sites 1969-1976. Space Weather, 2013, 11: 651–660
33 Zhou H, Li H T, Dong G L. Relative position determination between Chang'E-3 lander and rover using in-beam phase referencing. Sci China Inf Sci, 2015, 58: 1–10
34 Liu Z Q, Di K C, Peng M, et al. High precision landing site mapping and rover localization for Chang'E-3 mission. Sci China-Phys Mech Astron, 2015, 58: 1–11
35 Ye P J, Sun Z Z, Zhang H, et al. An overview of the mission and technical characteristics of Chang'E-4 Lunar Probe. Sci China Tech Sci, 2017, 60: 658–667
36 Ye P J, Sun Z Z, Rao W, et al. Mission overview and key technologies of the first Mars probe of China. Sci China Tech Sci, 2017, 60: 649–657